

Alizarin red removal using epichlorohydrin-modified walnut shells

Yinghua Song*, Ying Zhang, Lin Zhuo

Department of Chemistry and Chemical Engineering, Chongqing Technology and Business University, Chongqing, China, Tel. +86-023-62769785; Fax: +86-023-62769785;

* To whom correspondence should be addressed. E-mail: yhswjyhs@126.com

ABSTRACT: This study investigated the adsorption of alizarin red (AR) from aqueous solutions using epichlorohydrin-modified walnut shells (EMWS). Through static adsorption experiments, the impact of contact time (t_c), initial pH of the solution, solution concentration (c_0), and temperature (T) on the adsorption of AR onto the EMWS was examined. The optimum values of t_c and pH were determined to be 360 min and 3.51, respectively. The adsorption capacity of the EMWS for AR increased when c_0 and T were increased. Non-linear fitting of the equilibrium data was performed using the Langmuir, Freundlich, and Temkin isotherms. AR adsorption was well explained by the Langmuir isotherm with the q_m of 81.44 mg / g at 323 K. To simulate the adsorption kinetics, various models including pseudo-first-order, pseudo-second-order, intra-particle diffusion, and Elovich models were employed. The results indicated that it followed the PSO kinetic model ($k = 4.56 \times 10^{-4}$ g / (mg·min), $q_e = 18.84$ mg / g and $R^2 = 0.9808$). Moreover, the Elovich model confirmed the occurrence of chemisorption. According to thermodynamic investigations, the adsorption of AR is found to be spontaneous ($\Delta G < 0$) and endothermic ($\Delta H = 12.24$ kJ / mol) while exhibiting an increase in entropy ($\Delta S = 58.5$ J / (mol·K)). The results indicated that EMWS showed great potential as an affordable and efficient adsorbent for treating AR wastewater.

KEYWORDS: Walnut shell; Alizarin red; Adsorption; Isotherm; Thermodynamics; Kinetics

INTRODUCTION

Large quantities of dye-containing wastewater have been discharged from various industrial activities, including printing and dyeing, textiles, food, leather, paper, and others. Wastewater containing dye must be specifically treated to reduce its harm to the environment before it is discharged. The treatment and reuse of such wastewater has always been an important issue in the wastewater treatment field. In the dye family, anthraquinone dyes are the second most common. Due to their vibrant colors, excellent color retention, and impressive color durability, they are widely used in the colorization of various textiles [1]. Traditionally used as an anthraquinone dye in textiles, alizarin red (AR) has the formula $C_{14}H_7NaO_7S$. Regrettably, the complex aromatic ring structure of AR makes it highly resistant to degradation, posing a serious impact on the environment and potentially jeopardizing human health as a result of its elevated toxicity, teratogenicity, and carcinogenicity. Studies have shown it can cause skin disorders, allergies, vision defects, and mutagenic effects [2]. Consequently, removing AR from dye-containing wastewater has attracted considerable attention.

There are several methods for removing AR, including photocatalytic degradation [3], electrochemical degradation [4], and adsorption techniques [2]. Of all these treatments, adsorption is superior to others in terms of its uncomplicated design, operational ease, and affordability [5].

Numerous cheaper and more effective adsorbents have now been developed from a variety of raw materials to treat dye-containing wastewater, including lemon peel [6], bamboo [7], pine bark [8], walnut wood [9], and orange peel [10], among others. These natural materials offer an alternative to adsorption technology to achieve its goals of low cost and environmental protection.

Walnut shell, a common agricultural byproduct, is often incinerated or simply discarded, producing large amounts of exhaust gas and dust that are harmful to the environment. Because of its excellent adsorption properties, good chemical stability, high mechanical strength, wide-ranging sources, and low cost, it is considered an effective adsorbent for treating organic contaminants in wastewater, such as malachite green [11], methylene blue [12], sunset yellow [13], Congo red [14], and dimethyl sulfide [15]. Walnut shells can be chemically modified with epichlorohydrin/diethylenetriamine [16] and formaldehyde [17] to improve their adsorption properties.

A preliminary study showed that raw walnut shells rarely, if ever, adsorb AR. To enhance its adsorption properties towards AR, a novel adsorbent was developed in this study by incorporating epichlorohydrin into the raw walnut shell to enhance its ability to adsorb AR. Compared to the unmodified walnut shell, the EMWS exhibited a 30-fold increase in its adsorption capacity for AR. AR dye removal was investigated of factors including the solution pH, concentration, contact time, and temperature. To uncover the characteristics of AR adsorption on EMWS, an analysis of non-linear isotherms and kinetics was conducted. The Langmuir isotherm explained the AR adsorption well. In addition, the adsorption of AR exhibited the kinetics of pseudo-second-order. Furthermore, the Elovich kinetic model supported chemisorption. This work aims to develop an adsorbent from raw walnut shells that can be used to treat dye-containing wastewater cost-effectively and efficiently.

MATERIALS AND METHODS

Materials

Chongqing Chuandong Chemical Co., LTD, China provided hydrochloric acid (HCl), sodium hydroxide (NaOH), and epichlorohydrin. Chengdu Kelong Chemical Reagent Co., LTD, China sold AR. To prepare the working solution, the required concentration (100-400 mg / L) was achieved by dissolving 0.4 g AR powder in 1000 mL deionized water to obtain the stock solution, which was then diluted.

Scheme 1 shows the chemical structure of AR.

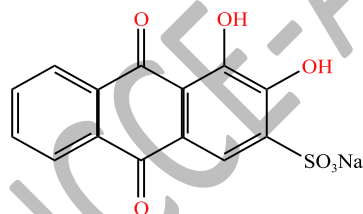


Fig. 1: Chemical structure of AR

Preparation of EMWS

Raw walnut shell was collected from local markets as agricultural waste in Chongqing, China. A thorough wash with deionized water was performed to remove dirt and other substances that dissolve in water. After that, it was dried in an oven at 50°C for 24 hours. Subsequently, it was crushed with a stone grinder and sifted to obtain different particle sizes. Initial experimental investigations have indicated that the adsorption capacity of AR on EMWS

exhibits minimal variation across different particle sizes. However, it should be noted that excessively small particle sizes of the adsorbent may impede the subsequent separation process. Consequently, for this study, the adsorbent with a particle size ranging from 375-250 μ m was chosen.

A method resembling the one explained by Y.H. Song et al. was employed to chemically modify the walnut shell with epichlorohydrin [10]. The epichlorohydrin-modified walnut shell (EMWS) was prepared by the following processes. 2.0 grams of walnut shell, 45 milliliters of sodium hydroxide solution (1.25 mol / L), and 30 milliliters of the epichlorohydrin were mixed in a flask and heated at 40 $^{\circ}$ C for 6 hours. Afterward, the mixture underwent filtration and was rinsed with deionized water until the pH of the effluent was maintained at 6.5 ± 0.2 . Finally, the prepared adsorbent can be used after drying for 24 hours at 50 $^{\circ}$ C. The modification procedure can be represented as in Fig. 2 [18].

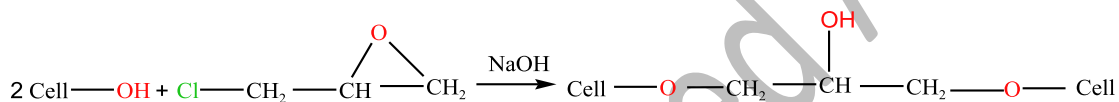


Fig. 2: The cross-linking reaction of EMWAS with epichlorohydrin

Adsorption studies

The impact factors, including the initial AR concentrations (200 - 400 mg / L), pH value (1.0 - 13.0), contact time (10 - 360 min), and temperature (303, 313, and 323 K), were assessed for AR adsorption on EMWS. Conical flasks were utilized for conducting batch experiments, with 0.4 g of EMWS and 100 mL of AR solution in each flask. To achieve a pH of 3.5 ± 0.1 , the solution underwent pH adjustment utilizing a pH meter (PB10, Sartorius, Germany) with either 1.0 mol / L hydrochloric acid or sodium hydroxide solution, except for the pH experiment. The AR concentration was determined at 430 nm spectrophotometrically (UV1102 Spectrophotometer, TECHCOMP, China). The data were obtained from three parallel experiments, whose averages were used for subsequent calculations to ensure precision.

Eq.1 was used to calculate the adsorption capacity, q (mg / g):

$$q = \frac{v(c_0 - c_t)}{m} \quad (1)$$

where c_0 and c_t (mg / L) are the initial AR concentration and the concentration at time t , respectively; v (L) is the solution volume; m (g) is the EMWS mass.

Equilibrium and kinetic data were fitted nonlinearly with the Microcal OriginPro 8.5 software.

RESULTS AND DISCUSSION

Effect of initial solution pH

The measurement of the zero charge point (pH_{pzc}) for the EMWS was conducted to investigate the impact of the initial solution pH [10]. The pH_{pzc} for the EMWS was determined to be 9.01 from Fig.3. It was observed that the EMWS surface exhibited positive charges below $\text{pH}_{\text{pzc}} = 9.01$, and negative charges above $\text{pH}_{\text{pzc}} = 9.01$ [19].

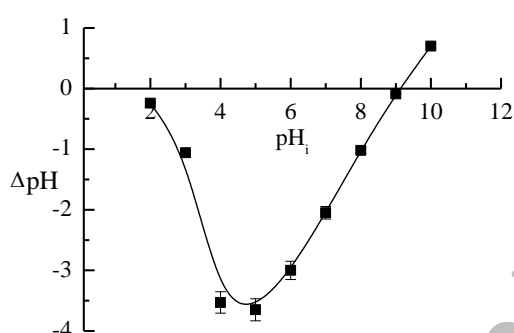


Fig. 3: *The pH of the zero charge point of EMWS*

As the pH increased, AR adsorption on the EMWS increased initially but then decreased (Fig.4). The highest adsorption was observed at a pH of 3.51. An anion exchange resin based on N-methylimidazolium has shown similar results for AR adsorption [20].

Low pH caused a reduction in the amount of anionic AR species available for interaction with the EMWS active sites due to a decrease in AR dissociation. AR molecules and the functional groups on the EMWS surface are electrostatically attracted to each other, which results in AR adsorption on the surface. As an anionic dye, the sulfonic acid groups ($-\text{SO}_3^-$) of AR are negatively charged in aqueous solutions. At a pH less than $\text{pH}_{\text{pzc}} = 9.01$, the surface of the EMWS was occupied by positively charged H^+ ions, which favored enhanced adsorption of the negatively charged AR on the surface. For $\text{pH} > \text{pH}_{\text{pzc}} = 9.01$, the adsorption capacity of AR noticeably declined as the EMWS surface became more negatively charged because of the electrostatic repulsion with the EMWS surface. Similar results were obtained for anionic dye adsorption on epichlorohydrin crosslinked chitosan/carbon clay [21].

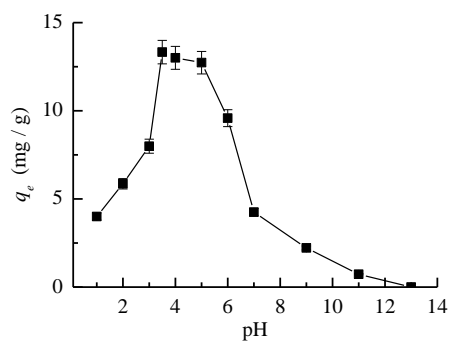


Fig.4: Effect of pH ($c_0 = 100 \text{ mg/L}$, $T = 303\text{K}$, EMWS dosage = 4 g/L , contact time = 6 h , rpm = 150)

Effect of contact time

As illustrated in Fig.5, the adsorption of AR depends on the contact time. With increasing time, the adsorption capacity steadily increased and eventually stabilized at about 300 minutes. A rapid AR adsorption occurred in the first 100 minutes due to the abundance of unoccupied adsorption locations on the EMWS surface, leading to the accelerated movement of AR from the bulk solution to the EMWS surface. As these vacancies became occupied, the adsorption rate gradually decreased [6]. Over time, the repulsive force between the solution and the AR molecule increased, hindering the adsorption of AR on the remaining vacancy sites. Similar findings have been obtained for Acid Orange 7 adsorption onto activated carbon [22].

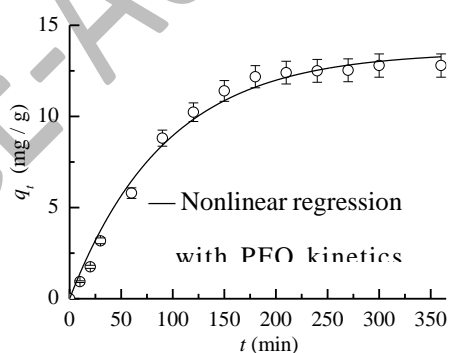


Fig. 5: Effect of contact time

($c_0 = 100 \text{ mg/L}$, $\text{pH} = 3.5 \pm 0.1$, $T = 303 \text{ K}$, EMWS dosage = 4 g/L , rpm = 150)

Adsorption isotherms

For this equilibrium system, the Langmuir (Eq. 2), Freundlich (Eq. 3), and Temkin (Eq. 4) nonlinear expressions were used [13].

$$q_e = \frac{q_{max}K_L c_e}{1+K_L c_e} \quad (2)$$

$$q_e = k_F c_e^{\frac{1}{n}} \quad (3)$$

$$q_e = \frac{RT}{b} \ln K_T + \frac{RT}{b} \ln c_e \quad (4)$$

where q_e (mg / g) is the equilibrium adsorption capacity, q_{max} (mg / g) is the Langmuir maximum adsorption capacity, c_e (mg / L) is the equilibrium AR concentration, K_L , K_F , and K_T are the Langmuir, Freundlich, and Temkin equilibrium constants (L / mg), respectively, n is a dimensionless constant, R (8.314 J / (mol·K)) is the ideal gas constant, T (K) is the absolute temperature, and b (J / mol) is the Temkin constant.

As the initial concentration of AR increased, so did the residual AR concentration and the adsorption capacity of AR on the EMWS (Fig. 6). For example, as the initial AR concentration was raised from 200 to 400 mg / L at 303 K, the residual AR concentration increased from 126.87 to 279.93 mg / L, and the adsorption capacity also escalated from 16.78 to 30.52 mg / g. At the same temperature, as the residual AR concentration increased, the driving force for mass transfer increased and the interaction force between AR and EMWS was enhanced, thus increasing the adsorption capacity of EMWS. The findings aligned with those described for AR adsorption onto a nano-composite of activated carbon and γ -Fe₂O₃ [23].

The adsorption capacity at equilibrium also rose for the same concentration as the temperature increased, as depicted in Fig.6. This indicated that the process of AR adsorption was endothermic. Similar results were reported for AR adsorption onto N-methylimidazolium anion exchange resin [20] and NiFe₂O₄/polyaniline magnetic composite [24].

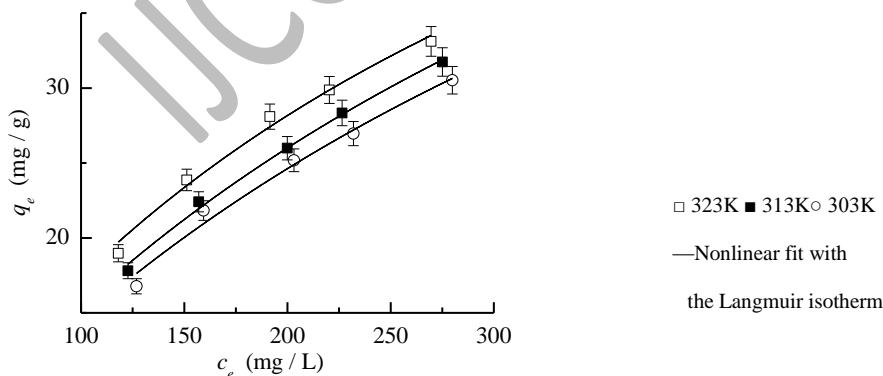


Fig. 6: Adsorption isotherms of AR onto EMWS

($pH = 3.5 \pm 0.1$, adsorbent dosage = 4 g / L, contact time = 6 h, rpm = 150)

Table 1 provides the adsorption parameters and coefficients of the nonlinear fits for the Langmuir, Freundlich, and Temkin models. The correlation coefficients obtained indicate that the three isotherm models are capable of achieving an ideal fit for AR adsorption on the EMWS. According to the Langmuir isotherm fitting, monolayer adsorption occurred at specific sites, and the adsorbed AR molecules experienced little interaction [25]. With the increase in temperature (303-323 K), q_m increased from 78.95 mg / g to 81.44 mg / g, suggesting that AR adsorption on EMWS was endothermic. The isotherm constants in Table 1 strongly advocated the relevance of the Freundlich isotherm in describing the AR-EMWS adsorption system, indicating the presence of physisorption coupled with chemisorption during the process [26]. The AR concentration at equilibrium and the adsorption capacity showed a favorable nonlinear relationship when values of n were greater than 1 [27]. The K_F was observed to increase with temperature, indicating that increasing temperature favored AR adsorption onto the EMWS. Previous studies have yielded similar findings regarding the adsorption of anionic dye on chitosan/carbon-clay crosslinked with epichlorohydrin [21]. According to the positive Temkin isotherm parameters, the adsorption of AR onto the EMWS was shown to be an endothermic process [28].

Table 1 Isotherms constants for AR adsorption on EMWS

T / K	Langmuir			Freundlich			Temkin		
	q_{max}	K_L	R^2	n	K_F	R^2	K_T	b	R^2
303	78.95	0.0023	0.9798	1.44	0.6152	0.9714	0.022	150.65	0.9883
313	80.09	0.0024	0.9950	1.46	0.6819	0.9890	0.023	152.74	0.9982
323	81.44	0.0031	0.9856	1.57	0.9584	0.9719	0.027	159.93	0.9886
313*	2.62	1.38	0.9532	1.41	1.79	0.9616	15.04	0.51	0.9399

*The equilibrium data of the raw walnut shell.

To assess the potential improvement in adsorption properties of the walnut shell through epichlorohydrin modification, the equilibrium adsorption of AR at 313K on the unmodified walnut shell was investigated and the results were given in Table 1. Compared to the unmodified walnut shell, the EMWS exhibited a 30-fold increase in its adsorption capacity for AR.

A comparison of q_m for different adsorbents was conducted in Table 2. The EMWS had a q_m of 80.09 mg / g for AR, comparable to that of other adsorbents. Adsorbents with higher q_{max}

than the EMWS such as NiFe₂O₄/polyaniline magnetic composite [24], and polyethyleneimine functionalized magnetic carbon nanotubes [30], are expensive as compared to the cheap walnut shells, and their preparation methods are more complex. The EMWS shows promise as a potential adsorbent for eliminating dyes from aqueous solutions.

Table 2 Adsorption Capacities of Various Adsorbents for AR

adsorbent	Langmuir <i>q_{max}</i> (mg / g)	T (°C)	References
Nano-composite (activated carbon / γ -Fe ₂ O ₃)	108.69	25	[23]
NiFe ₂ O ₄ /polyaniline magnetic composite	110	25	[24]
Polyaniline/carbon hybrids	7.61	40	[29]
Polyethyleneimine functionalized magnetic carbon nanotubes	196.08	25	[30]
Coal bottom ash-derived zeolite	15.25	25	[31]
Powdered activated carbon (PAC)	24.5	25	[32]
Nitric acid-treated PAC	57.8	25	[32]
Olive stone by-product	16.10	25	[33]
Mustard husk	1.97	25	[34]
Unmodified walnut shell	2.62	40	Present Work

Thermodynamic studies

A calculation of the free energy (ΔG), enthalpy (ΔH), and entropy (ΔS), can be made according to Eq.5[11].

$$\Delta G = (\Delta H - T\Delta S) = -RT \ln K_e \quad (5)$$

The key factor in determining the thermodynamic parameters in Eq.5 is how to properly calculate the value of K_e (which is dimensionless). A dimensionless K_e can be derived from K_L based on Y.H.Song's method [10]. In this present study, 0.4 grams WMWS was introduced into a solution of 100 millimeters, so K_e can be obtained by multiplying K_L by 4000 mg/L as shown in Eq.6 (Table 3).

$$K_e = 4000K_L \quad (6)$$

Table 3 displays the thermodynamic parameters obtained using Eq.5 and Eq.6. As demonstrated in Table 3, the values of the equilibrium constants used significantly impacted the calculated ΔG values. The ΔG derived from the dimensionless K_e was negative, indicating that AR adsorption on the EMWS was spontaneous [35], while the ΔG obtained by K_L directly was greater than zero, giving contradictory results about the spontaneity of the adsorption process. The ΔG values decreased with increasing temperature, indicating that adsorption feasibility is positively affected by the temperature [36]. AR adsorption on the EMWS was endothermic as indicated by the positive ΔH values. The adsorption ability was enhanced at elevated temperatures. At the same time, it also showed that in addition to physical adsorption, chemical reactions occurred during adsorption and the adsorption rate increased at higher temperatures. ΔS was greater than zero, reflecting the increased disorder of AR on the EMWS surface. Zeolites derived from coal bottom ash have shown similar results in AR biosorption [31].

Table 3 Thermodynamic properties for AR adsorption

<i>T</i> (K)	<i>K_L</i>	<i>K_e</i> (400 0 <i>K_L</i>)	ΔG (kJ / mol)		ΔH (<i>R</i> ²) (kJ / mol)	ΔS (J / (mol ·K))
			<i>K_L</i>	<i>K_e</i>		
3	0.0		15	-		
0	02	9.2	.3	5.		
3	3		0	5		
				9		
3	0.0		15	-	12.2	
1	02	9.6	.7	5.	4	58.5
3	4		0	8	(0.9	
				9	243)	
3	0.0		15	-		
2	03	12.4	.5	6.		
3	1		1	7		
				6		

Adsorption kinetics

Models of pseudo-first-order (PFO, Eq.7) [11], pseudo-second-order (PSO, Eq.8) [37], intra-particle diffusion (Eq.9) [11], and Elovich (Eq.10) [11] were examined to investigate the kinetic behavior of AR adsorption by EMWS.

$$q_t = q_e(1 - e^{-k_1 t}) \quad (7)$$

$$q_t = \frac{k_2 q_e^2 t}{1 + k_2 q_e t} \quad (8)$$

$$q_t = k_p t^{1/2} + C \quad (9)$$

$$q_t = \frac{1}{\beta} \ln(t) + \frac{1}{\beta} \ln(\alpha\beta) \quad (10)$$

Fit results for these models are shown in Table 4. Despite the correlation coefficient *R*² exceeding 0.98 for both PFO and PSO models, the *q_e* obtained by PSO deviated significantly from the experimental value. In contrast, the *q_e* derived by PFO was remarkably closer to the experimental value, the PFO model better described the kinetics of AR adsorption on EMWS. The Elovich model could also provide a good description of AR adsorption onto the EMWS since *R*² was 0.9757. Given

this, chemical interactions based on electron exchange or charge sharing occurred between AR and EMWS during this process. The R^2 value (0.9429) obtained from the intra-particle diffusion model presented in Table 4 suggests the presence of pore diffusion in AR adsorption. However, pore diffusion alone does not solely govern the diffusion rate, as liquid film diffusion also significantly contributes to the overall control of the diffusion process. These results were consistent with the previous studies on the adsorption of reactive red 120 anion dye onto chitosan-epichlorohydrin/zeolite [38] and the adsorption of AR onto polyaniline/carbon hybrids [29].

Table 4 Parameters of different kinetic models

Model	Parameters		
PFO	$k_1(1/\text{min}, 10^{-2})$	Rate constant	1.04
	$q_{e, cal} (\text{mg} / \text{g})$	Equilibrium capacity	13.79
	R^2	Correlation coefficient	0.9899
PSO	$k_2 (10^{-4}, \text{g} / (\text{mg}\cdot\text{min}))$	Rate constant	4.56
	$q_{e, cal} (\text{mg} / \text{g})$	Equilibrium capacity	18.84
	R^2	Correlation coefficient	0.9808
Elovich	$\alpha (\text{mg} / (\text{g}\cdot\text{min}))$	Rate constant	0.37
	$\beta (\text{g} / \text{mg})$	The Elovich constant	0.25
	R^2	Correlation coefficient	0.9757
Intra particle Diffusion	$k_p (\text{mg} / (\text{min}^{1/2}\cdot\text{g}))$	Rate constant	0.88
	$C (\text{mg} / \text{g})$	Model constant	-0.81
	R^2	Correlation coefficient	0.9429

$q_{e,exp}$ (mg / g)	Experimental data of the Equilibrium capacity
----------------------	--

CONCLUSIONS

The current study involved the modification of walnut shells using epichlorohydrin to prepare an economically viable EMWS with enhanced adsorption capabilities. The removal of anionic AR dye by EMWS was evaluated by batch adsorption experiments. The results indicated that the adsorption of AR was influenced by various factors, including the solution pH, contact time, temperature, and initial AR concentration. AR adsorption was well explained by the Langmuir isotherm with the q_m of 80.09 mg / g at 313 K, compared to 2.62 mg / g for the unmodified walnut shell as an adsorbent. Furthermore, AR adsorption onto the EMWS was explained using kinetics, which indicated that it followed the PSO kinetic model. Additionally, the Elovich model confirmed the occurrence of chemisorption. The thermodynamics of the adsorption process demonstrated that AR adsorption onto the EMWS was both spontaneous and endothermic. However, it is imperative to further investigate the impact of humus compounds, as well as other anions and cations present in wastewater, on the practical applications of the EMWS for AR adsorption. Consequently, the EMWS exhibits potential as an economical and effective adsorbent for eliminating anionic AR dye from aqueous solutions. Additionally, these chemically modified biomaterials can be explored for the removal of other dye contaminants.

REFERENCES

- [1] Zhang, Z., Chen, H., Wu, W., Pang, W., Yan, G., [Efficient removal of Alizarin Red S from aqueous solution by polyethyleneimine functionalized magnetic carbon nanotubes](#), *Bioresource Technol.*, **293**:122100 (2019).
- [2] Gollakota, A.R.K., Munagapati, V.S., Volli, V., Gautam, S., Wen, J.C., Shu, C.M., [Coal bottom ash derived zeolite \(SSZ-13\) for the sorption of synthetic anion Alizarin Red S \(ARS\) dye](#), *J. Hazard. Mater.*, **416**:125925 (2021).

- [3] Akshatha, S., Sreenivasa, S., Parashuram, L., Kumar, V. U., Sharma, S.C., Nagabhushana, H., Kumar, S., Maiyalagan, T., [Synergistic effect of hybrid Ce³⁺/Ce⁴⁺ doped Bi₂O₃ nano-sphere photocatalyst for enhanced photocatalytic degradation of alizarin red S dye and its NUV excited photoluminescence studies](#), *J. Environ. Chem. Eng.*, **7**: 103053(2019).
- [4] Ritesh, P., Vimal, C.S., [Understanding of ultrasound enhanced electrochemical oxidation of persistent organic pollutants](#), *J. Water Process. Eng.*, **37**:101378(2020).
- [5] Okoye, C.C., Onukwuli, O.D., Okey-Onyesolu, C.F., [Utilization of salt activated Raphia hookeri seeds as biosorbent for Erythrosine B dye removal: Kinetics and thermodynamics studies](#), *J. King Saud Univ.- Sci.*, **31**:849-858(2019).
- [6] Makhwedzha, D.R., Mavhungu, A., Moropeng, M.L., Mbaya, R., [Activated carbon derived from waste orange and lemon peels for the adsorption of methyl orange and methylene blue dyes from wastewater](#), *Heliyon.*, **8**: e09930(2022).
- [7] Tulashie, S.K., Kotoka, F., Botchway, B. N., Adu, K., [Removal of reactive violet 5 azodye \(V5R\) using bamboo, and calabash biochar](#), *Heliyon.*, **8**:e10908(2022).
- [8] Zawahreh, K. A., Barral, M.T., Al-Degs, Y., Paradelo, R., [Competitive removal of textile dyes from solution by pine bark-compost in batch and fixed bed column experiments](#), *Environ. Technol. Innov.*, **27**:102421(2022).
- [9] Hajatia, S., Ghaedib, M., Mazaheri, H., [Removal of methylene blue from aqueous solution by walnut carbon: optimization using response surface methodology](#), *Desalin. Water Treat.* **57**:3179-3193(2016).
- [10] Song, Y., Peng, R., Chen, S., [Malachite green adsorption from aqueous solution by epichlorohydrin modified orange peel](#), *Fresen. Environ. Bull.*, **30(04A)**:4569-4577(2021).
- [11] Song, Y., Chen, S., Xu, H., [Treatment of Malachite Green Wastewater Using Walnut Shell](#), *Desalin. Water Treat.*, **228**:422-430(2021).
- [12] Miyaha, Y., Lahrichi, A., Idrissi, M., Khalil, A., Zerrouq, F., [Adsorption of methylene blue dye from aqueous solutions onto walnut shells powder: Equilibrium and kinetic studies](#), *Surf. Interfaces.*, **11**:74-81(2018).

- [13] Song, Y., Peng, R., Gou, L., Ye, M., [Removal of Sunset Yellow by Methanol Modified Walnut Shell](#), *Iran. J. Chem Chem. Eng.*, **40(4)**: 1095-1104(2021).
- [14] Li, Z., Hanafy, H., Zhang, L., Sellaoui, L., Netto, M.S., Oliveira, M.L.S., Seliem, M.K., Dotto, G. L., Petriciolet, A.B., Li, Q., [Adsorption of Congo red and methylene blue dyes on an ashitaba waste and a walnut shell-based activated carbon from aqueous solutions: Experiments, characterization and physical interpretations](#), *Chem. Eng. J.*, **388**:124263(2020).
- [15] Jalilvand, H., Feyzi, F., Dehghani, M. R., [Adsorption of dimethyl sulfide from model fuel on raw and modified activated carbon from walnut and pistachio shell origins: Kinetic and thermodynamic study](#), *Colloid. Surfaces A*. **593**:124620(2020).
- [16] Cao, J., Lin, J., Fang, F., Zhang, M., Hu, Z., [A New Adsorbent by Modifying Walnut Shell for the Removal of Anionic Dye: Kinetic and Thermodynamic Studies](#), *Bioresource Technol.*, **163**:199-205(2014).
- [17] Song, Y., Zhuo, L., Xu, H., Ye, M., [Congo Red adsorption from aqueous solution by formaldehyde modified walnut shell](#), *Fresen. Environ. Bull.* **31(01A)**:1093-1102(2022).
- [18] Udoetoka, I., Dimmicka, R.M., Wilson, L.D., Headley, J.V., [Adsorption properties of cross-linked cellulose-epichlorohydrin polymers in aqueous solution](#), *Carbohydr. Polym.*, **136**:329-340(2016).
- [19] Eletta, O.A.A., Ajayi, O.A., Ogunleya, O.O., Akpan, I.C., [Adsorption of cyanide from aqueous solution using calcinated eggshells: Equilibrium and optimization studies](#), *J. Environ. Chem. Eng.*, **4**:1367-1375(2016).
- [20] Zhang, Z., Zhu, L., Lu, W., Li, X., Sun, X., Lü, R., Ding, H., [Evaluation of functional group content of N-methylimidazolium anion exchange resin on the adsorption of methyl orange and alizarin red](#), *Chem. Eng. Res. Des.*, **111**:161-168 (2016).
- [21] Marrakchi F., Hameed B.H., Hummadi E.H., [Mesoporous biohybrid epichlorohydrin crosslinked chitosan/carbon-clay adsorbent for effective cationic and anionic dyes adsorption](#), *Int. J. Biol. Macromol.*, **163**:1079-1086(2020).

- [22] Bouzikri, S., Ouasfi, N., Khamliche, L., [Bifurcaria bifurcata activated carbon for the adsorption enhancement of Acid Orange 7 and Basic Red 5 dyes: Kinetics, equilibrium and thermodynamics investigation](#), *Energy Nexus.*, **77**:100138(2022).
- [23] Fayazi, M., Ghanei-Motlagh, M., Taher, M.A., [The adsorption of basic dye \(Alizarin red S\) from aqueous solution onto activated carbon/ \$\gamma\$ -Fe₂O₃ nano-composite: Kinetic and equilibrium studies](#), *Mat. Sci. Semicon.Proc.*, **40**:35-43(2015).
- [24] Liang, Y., He, Y., Zhang, Y., Zhu, Q., [Adsorption property of alizarin red S by NiFe₂O₄/polyaniline magnetic Composite](#), *J. Environ. Chem. Eng.*, **6**: 416-425 (2018).
- [25] Dada, A.O., Adekola, F.A., Odebunmi, E.O., Dada, F.E., Bello, O.M., Akinyemi, B.A., Bello, O.S., Umukoro, O.G., [Sustainable and low-cost ocimum gratissimum for biosorption of indigo carmine dye: kinetics, isotherm, and thermodynamic studies](#), *Int. J. Phytoremediat.*, **22(14)**:1524-1537(2020a).
- [26] Davoudi, S., [Adsorption of Methylene Blue \(MB\) Dye Using NiO-SiO₂NPs Synthesized from Aqueous Solutions: Optimization, Kinetic and Equilibrium Studies](#), *Iran. J. Chem. Chem. Eng.*, **41(7)**:2343-2357(2022).
- [27] Baloo, L., Isa, M.H., Sapari, N.B., Jagaba, A.H., Wei, L.J., Yavari, S., Razali, R., Vasu, R., [Adsorptive removal of methylene blue and acid orange 10 dyes from aqueous solutions using oil palm wastes-derived activated carbons](#), *Alex. Eng. J.* **60**:5611-5629 (2021).
- [28] Geremew, B., Zewde, D., [Hagenia abyssinica leaf powder as a novel low-cost adsorbent for removal of methyl violet from aqueous solution: Optimization, isotherms, kinetics, and thermodynamic studies](#), *Environ. Technol. Innov.* **28**: 102577(2022).
- [29] Zhou J., Sun Y., Zhou C., Sun X., Han J., [Polyaniline/carbon hybrids: Synthesis and application for alizarin red S removal from water](#), *Colloid. Surface. A*, **676**:132204(2023).
- [30] Zhang Z., Chen H., Wu W., Pang W., Yan G., [Efficient removal of Alizarin Red S from aqueous solution by polyethyleneimine functionalized magnetic carbon nanotubes](#), *Bioresource Technol.*, **293**:122100(2019).
- [31] Gollakota, A. R.K., Munagapati V.S., Volli, V., Gautam, S., Wen, J.C., Shu, C.M., [Coal bottom ash derived zeolite \(SSZ-13\) for the sorption of synthetic anion Alizarin Red S \(ARS\) dye](#), *J. Hazard. Mater.*, **416**:125925(2021).

- [32] Kamarehie, B., Jafari, A., Ghaderpoori, M., Karami, M.A., Mousavi, K., Ghaderpoury, A., [Data on the alizarin red S adsorption from aqueous solutions on PAC, treated PAC, and PAC/ \$\gamma\$ Fe₂O₃](#), *Data Brief*, **20**:903-908(2018).
- [33] Albadarin, A.B., Mangwandi, C., [Mechanisms of Alizarin Red S and Methylene blue biosorption onto olive stone by-product: isotherm study in single and binary systems](#), *J. Environ. Manage.*, **164**: 86-93(2015).
- [34] Gautam, R.K., Mudhoo, A., Chattopadhyaya, M.C., [Kinetic, equilibrium, thermodynamic studies and spectroscopic analysis of Alizarin Red S removal by the mustard husk](#), *J. Environ. Chem. Eng.*, **1**:1283-1291(2013).
- [35] Skwierawska, A.M., Bliźniewska, M., Muza, K., Nowak, A., Nowacka, D., Syeda, S. E. Z., Khan, M.S., Łęska, B., [Cellulose and its derivatives, coffee grounds, and cross-linked, \$\beta\$ -cyclodextrin in the race for the highest sorption capacity of cationic dyes in accordance with the principles of sustainable development](#), *J. Hazard. Mater.*, **439**:129588(2022).
- [36] Pandey, D., Daverey, A., Dutta, K., Yata, V.K., Arunachalam, K., [Valorization of waste pine needle biomass into biosorbents for the removal of methylene blue dye from water: Kinetics, equilibrium and thermodynamics study](#), *Environ. Technol. Innov.*, **25**:102200(2022).
- [37] Ho, Y. S., McKay, G., [Pseudo-second order model for sorption processes](#), *Process Biochem.* **34**: 451-465(1999).
- [38] Jawad, A.H., Abdulhameed, A. S., Reghioua, A., Yaseen, Z.M., [Zwitterion composite chitosan-epichlorohydrin/zeolite for the adsorption of methylene blue and reactive red 120 dyes](#), *Int. J. Biol. Macromol.*, **163**:756-765(2020).